JOURNAL OF AIRCRAFT
Vol. 44, No. 1, January–February 2007

Dynamics of Corotating Vortex Filaments Part 2: Experimental Results

Linda K. Kliment,* Teresa S. Miller,* and Kamran Rokhsaz†
Wichita State University, Wichita, Kansas 67260-0044

DOI: 10.2514/1.22230

The interactions of pairs of corotating vortex filaments have been investigated experimentally in a water tunnel. The time history of the motion of each filament has been recorded at several downstream locations to analyze its spatial and temporal behavior. Two sets of data are presented in which the vortices have been excited over a range of frequencies using a shaker. The excitation frequency and its multiples have been shown to be present in the downstream flow. At each downstream position, the filaments have been shown to move along preferred directions, suggesting their tendency to form planar waves, inclined relative to the line connecting them. The amplitudes of these waves have been shown to grow, implying unstable interaction between the vortices. The angles of the planes containing the motion have been presented and compared with the predictions of two analytical models. The scatter in the data prevented quantitative comparison with the analytical predictions. However, the flow is shown to contain all of the essential features predicted by two analytical models.

Nomenclature

a	=	exponential growth rate
b	=	distance between blades
b_v	=	vortex span
C	=	chord length
c	=	core radius
f	=	excitation frequency, Hz
$I_{\min}$, $I_{\max}$	=	principal second moments of vortex position
n	=	order of the ellipse
Re_v	=	vortex Reynolds numberΓ/ν
V_∞	=	freestream velocity
x, y, z	=	coordinate axes
y_C, z_C	=	coordinates of the centroid
α	=	angle of attack or nondimensional amplitude growth rate $=(2\pi b^2/\Gamma)a$
β	=	nondimensional wave number $=\lambda b_v$
Γ	=	circulation
δ	=	nondimensional self-induction cutoff distance
θ	=	inclination angle of the plane of motion
λ	=	wave number
ω	=	frequency of spiraling (i.e., orbiting)

Introduction

RECENTLY, the kinematics of corotating longitudinal vortex filaments, that are typical of those emanating from wing tips and flap tips, has become the subject of renewed interest. Efforts at better understanding the behavior of these flowfields have been driven by more powerful computational tools, modern analytical models, and recent discoveries suggesting new mechanisms for wake vortex self-destruction [1–4]. Of particular interest has been the merger process by which corotating vortices combine into a single coherent structure. The stability of this flow type and its merger process have been studied extensively from the viewpoint of viscosity and vortex diffusion, in two- [5–8] and three-dimensional sense [9–14].

The two-dimensional solutions revolve around the effects of viscosity and diffusion of one vortex by the strain field of the other. Dritschel and Legras [5] arrived at approximate equations for the evolution of vortices in a general strain field and extended their model to include disturbances to the elliptical shape of each contour. They also showed good agreement between their analytical model and numerical solutions. Meunier et al. [6] proposed a quantitative criterion for the merging of a pair of equal two-dimensional corotating vortices and validated their conclusions experimentally. They arrived at criteria for merger that depended on the shape of vorticity distribution, based on the global impulse quantities. Le Dizès and Verga [7] used two-dimensional direct numerical simulation over a wide range of Reynolds numbers to identify two phases for the merger. They showed that in the first phase, each vortex adapts to the strain field of the other in an inviscid manner, whereas the second phase is dominated by viscous diffusion. In a related work, Meunier and Villermaux [8] showed that the advection of a passive scalar blob in the deformation field of an axisymmetric vortex is a simple mixing problem. The blob rolls up in a spiral which ultimately fades away in the diluting medium.

Three-dimensional analyses include the kinematics of the self- and mutual-induction effects. Bertenyi and Graham [9] considered the merger of corotating aircraft wake vortices experimentally. They observed that filaments of equal strength coorbited while drawing closer to each other, before merging quickly. They showed that with the proper choice of nondimensional variables, the distance to merger, for a given initial separation, would collapse onto a single curve. Meunier and Leweke [10] investigated the interactions of two vortex filaments of equal strength experimentally. They observed that at low Reynolds numbers, the vortices behave similar to those in two-dimensional flow and merge when their core sizes exceed approximately 30% of the vortex span. At higher Reynolds numbers, they observed ellipticlike three-dimensional instabilities leading to merger at smaller individual core sizes than in two-dimensional flow. Le Dizès and Laporte [11] developed an analytical model for analyzing the interactions of two parallel Gaussian vortices. They showed that this system exhibits elliptical instability due to elliptic deformation of the vortex cores. The motion associated with this instability was shown to be periodic with a preferred direction. They also validated their results using direct numerical simulation. Laporte and Leweke [12] used closely spaced *counter*-rotating vortices in a water tank to investigate elliptic instability. They showed that the growth rate of such instabilities is higher than that of Crow. They also validated their results computationally. Cerretelli and Williamson

Presented as Paper AIAA-2004-2434 at the 34th AIAA Fluid Dynamics Conference and Exhibit, Portland, OR, 28 June–1 July 2004; received 3 January 2006; revision received 4 July 2006; accepted for publication 10 July 2006.

*Graduate Research Assistant, Student Member of AIAA.
†Professor, Associate Fellow of AIAA.

[13] investigated the structure of the vorticity field that causes the corotating vortices to be pushed toward each other during merger. They showed that such a flowfield contains two counter-rotating vortices whose induced velocities push the main vortices together.

Although most of the efforts listed above were focused on the viscous effects, certain solutions have also been offered for purely kinematic interaction between corotating vortices. Examples of two-dimensional models include those of Hassan [15], Eckhardt [16], and Saffman [17] who investigated stability of the interactions among multiple vortices. The classical three-dimensional model for studying the stability of corotating longitudinal vortex filaments has been that of Jimenez [18]. This analysis, which was based on the Biot–Savart law and resembled that of Crow [19], indicated that such interactions are generally stable, except over narrow ranges of wave number. However, Miller et al. [20] arrived at results that were opposite to those of Jimenez. Their model, which was also based on the Biot–Savart law, indicated that corotating vortex filaments tend to oscillate along preferred directions with increasing amplitude, rendering the motion widely *unstable*, except for very narrow bands of wave number. The preferred direction of motion predicted by this analysis, while on the same order of magnitude, did not agree entirely with that offered by Le Dizès and Laporte [11]. The latter results were verified by direct numerical solution, but other forms of verification have been rare. Jacob et al. [21–23] who performed a large set of experiments with corotating vortex filaments did not offer any data about the time-dependent motion of the filaments or their preferred directions of motion. Kliment [24] and Rokhsaz and Kliment [25] who studied this type of motion in a water tunnel observed a preferred direction of vortex motion in some cases. However, their results concerning the angles and the rates of growth of the amplitude were inconclusive because in their experiments the vortices were excited only by the background turbulence as opposed to single excitation frequencies.

In the present paper, the authors report on their experimental investigation of the time-dependent interactions of a pair of corotating vortex filaments when forced to oscillate at predetermined frequencies. The experiments have been performed in a water tunnel, and the time-dependent motion of the filaments is recorded using a previously reported optical technique [26]. It is shown that the motion indeed exhibits a preferred direction when the filaments are excited at predominant frequencies. The angles of the planar standing waves measured in this investigation are compared to the analytically predicted values. Also, estimates are made for the growth rate of the amplitude of motion.

Theoretical Models

Elliptic Instability

In the interest of completeness, a brief explanation of the elliptic instability is provided in this section. The reader is urged to consult Le Dizès and Laporte [11] for complete details.

Le Dizès and Laporte modeled each filament by a Gaussian vortex. The vortices could be counter- or corotating. In the latter case, the vortices would orbit at a constant rate. Subtracting the effect of the orbiting would result in the flowfield of a stationary pair of corotating vortices, each imposing a strain field on the other. The stability could be determined by introducing small spatially periodic perturbations on the streamlines of each vortex and expanding most nonlinear terms to their leading term. They showed that the filaments would form planar waves inclined relative to the line connecting them. They also arrived at an expression for the growth rate of the amplitude of motion.

Mutual Induction

The details of this analytical approach were reported by Miller et al. [20]. However, a brief explanation of the method is furnished here.

The formulation of this model followed that of Crow [19] very closely in the Biot–Savart law and was employed to examine the mutually induced natural oscillations of a pair of corotating vortex filaments. A cutoff distance was employed to remove the strong singularity in the self-induction term. In certain parts of the state space, the effect of the magnitude of the cutoff distance on the amplitude and the direction of motion could be quite large.

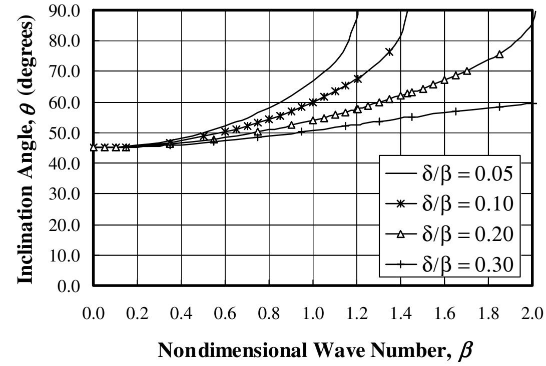

Fig. 1 Analytically predicted preferred direction of motion for antisymmetric mode (Miller et al.).

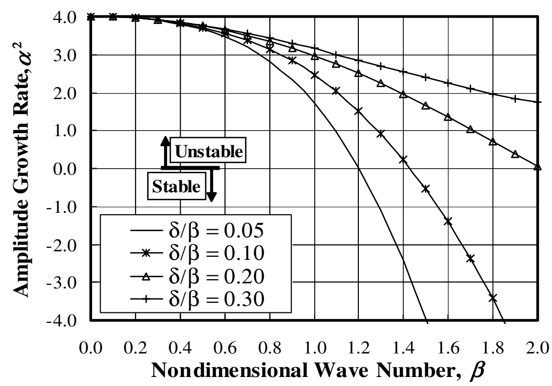

Fig. 2 Growth rate of the amplitude of the antisymmetric mode (Miller et al.).

The filaments were shown to form planar waves, inclined relative to the line connecting their mean positions. The waves, which were stationary relative to the freestream, could assume one of two modes. While the symmetric mode proved to be stable over a wide range of wave numbers, the antisymmetric mode was shown to be mostly unstable. Over the range of wave numbers conducive to strong Crow instability, the standing waves of the antisymmetric mode were shown to be inclined at approximately 45–90 deg relative to the line connecting their mean positions, as shown in Fig. 1. Furthermore, the waves were proven to be unstable over a wide range of wave numbers as indicated in Fig. 2. In this figure, α represents the eigenvalues used for stability analysis. Therefore, positive values indicate regions of instability. It is obvious from this figure that, according to this method of analysis, the antisymmetric mode is unstable for the most part. Furthermore, the degree of instability depends on the magnitude of the cutoff distance.

Experimental Method

The work described here was performed in the water tunnel at the National Institute for Aviation Research (NIAR), located on the campus of Wichita State University (WSU). This facility is a closed-loop horizontal tunnel containing approximately 13,250 liters (3500 gal) of water. The clear test section, visible from five directions, is 0.61 m (2 ft) deep, 0.91 m (3 ft) high, and 1.83 m (6 ft) long. A 0.76-m (2.5 ft) segment with constant cross-sectional area connects the test section to the diffuser. This section can also be used as an extension of the test section, allowing observation of a vortex filament over a length of approximately 2.45 m (8 ft). Water speed can be varied from 0.015 m/s (0.05 ft/s) to 0.305 m/s (1.0 ft/s), corresponding to flow Reynolds numbers of 16,500 to 3.3×10^5 per

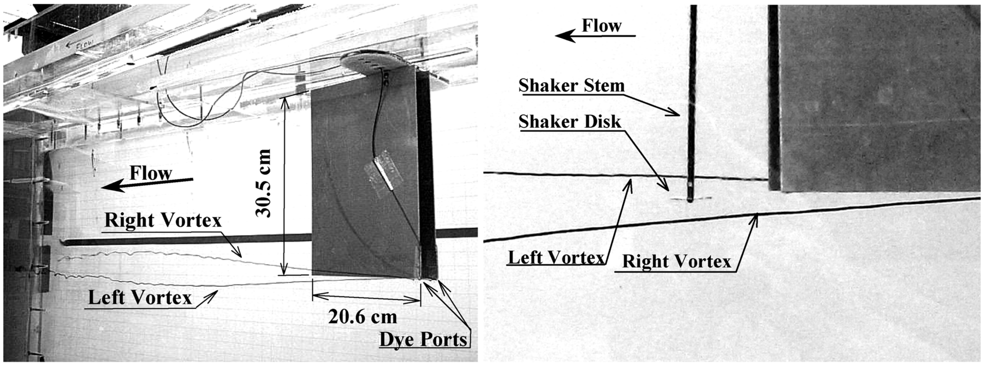

a) Overall view b) Close up view of the shaker

Fig. 3 Vortex generating blades in the tunnel.

meter (5000–100,000 per foot), with very low levels of turbulence. However, the speeds of 0.06 to 0.18 m/s (0.2 to 0.6 ft/s) contain the least amount of turbulence, and therefore, are most suitable for flow visualization.

The experimental apparatus used for this research was almost identical to that reported by Rokhsaz et al. [27] and is shown in Fig. 3. Vortex generation was accomplished by using two rectangular flat blades, mounted on a reflection plane that was located approximately 7.6 cm (3 in.) below the free surface of the water. Each blade was made of 1.6 mm (1/16 in.) thick aluminum with a chord length and a span length of 20.6 cm and 30.5 cm (8.1 in. and 12 in.), respectively. The blade incidence angles could be set independently for any arbitrary distance between the two vortex filaments. This arrangement allowed controlling the vortex strengths and the vortex span independently. For the purpose of the present study, the blade angles of attack were set such as to generate vortex filaments that rotated in the same direction. Vortex strength could also be varied via tunnel flow speed.

A shaker was added to the apparatus to introduce excitations of known frequency at fixed amplitude into the flow. The primary mechanism for moving the vortices was a thin circular disk with a radius of 1.9 cm (0.75 in.) placed between the filaments and parallel to the freestream just downstream of the trailing edge of the blades. This disk was moved harmonically parallel to the blades' span and normal to the flow with the amplitude of ±2.5 mm (±0.1 in.).

The data acquisition was identical to that reported by Kliment [24] in that the vortex filaments were visualized using a water–milk–alcohol mixture. The cross sections of the vortices were illuminated at fixed downstream distances using a white light sheet. At each downstream distance, the motion was digitally recorded at 30 Hz, from which the time-dependent deviations of the filaments from their mean positions could be extracted. The frequency content of the motion was identified using a fast Fourier transform (FFT) of this data. Also, the preferred direction of vortex motion could be discerned quantitatively from the second moments of the instantaneous positions relative to the mean vortex location.

The data acquisition technique described here allowed recording the time history of the vortex motion as long as the visualization mixture remained in the core. Therefore, quantitative data could not be obtained close to the merger where the vortices were severely strained.

Likewise, vigorous shaking of the filaments, in frequency or amplitude, resulted in dispersion of the visualization mixture, which prevented data acquisition as well. This limited the experimental investigation to nondimensional wave numbers below 1.4.

Results and Discussion

Two cases were studied that had the same blade separation distance, but with different angles of attack and tunnel speeds. The physical parameters associated with these cases are given in Table 1. Data were acquired at three locations downstream of the blades. The closest distance was chosen sufficiently far from the blades to allow a complete roll up of the wake, while the longest distance was dictated by the size of the tunnel and the merger location. The blades' angles of attack were set to produce corotating filaments of approximately equal strength. This was accomplished visually by forcing the center of orbiting to be near halfway between the two filaments. Consequently, it was not possible to ensure exact equality of the vortex strengths. The resulting vortex Reynolds numbers varied from 2000 to 3200. The reader is cautioned that the data presented in this paper contain all of the measurements made, without exception. Although it is logical to conclude that some of the data are in error, at this writing, the authors have no way of knowing which points are in error and which parts are more reliable.

A typical time exposure of the vortex core position at one downstream location is shown in Fig. 4. In this figure, within the clouds, each point represents the instantaneous location of the vortex filament in one video frame on that side. Each cloud consists of approximately 4200 points. The preferred direction of motion is clearly obvious in Fig. 4. However, these angles were not as evident visually in every case because their associated clouds formed more of a circular pattern than an oblong one. A measure of the clarity of the degree to which a cloud deviated from a circular shape was the ratio of the second moments of the instantaneous vortex position (i.e., moment of inertia) relative to its mean location. Figure 5 shows this quantity over the full range of wave numbers and downstream distances. It is obvious from this figure that in the majority of the cases, the maximum moment of inertia was approximately 1.5–2.0 times the minimum moment of inertia. Therefore, in the majority of the cases, the vortices exhibited a distinct preferred direction of motion. The reader is cautioned that Figs. 5a and 5b have been plotted with different scales on the ordinate.

The inclination angles of the planes containing the motion are shown in Fig. 6, where for the purpose of comparison, the analytically predicted values for elliptic instability are also shown. The latter values were obtained from Eq. 5.13 of [11], given here for clarity,

Table 1 Parameters used in the experiments

Parameter	Value
Blade size	20.6 by 30.5 cm
Blade separation	7.62 cm
Downstream locations (x/C)	3.70, 4.44, 5.19
Excitation frequency	0.0–1.6 Hz
Flow speed	
Case 1	0.085 m/s
Case 2	0.100 m/s
Angles of attack (left, right)	
Case 1	7.5, 8.5 deg
Case 2	8.0, 8.0 deg
Vortex strength (left, right)	
Case 1	19.14, 21.55 cm^2/s
Case 2	18.77, 14.49 cm^2/s
Orbiting rate	
Case 1	0.135 rad/s
Case 2	0.119 rad/s

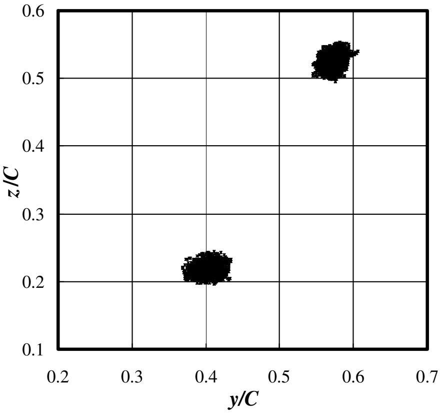

Fig. 4 Time exposure of the core position. Case 1, $x/C = 3.70$ cm; $\beta = 0.36$.

$$\cos(\theta) = \frac{1}{2} - \frac{(2.26 + 1.69n) - \lambda c}{14.8 + 9n} \quad (1)$$

In this expression, $n = 2$ corresponds to an ellipse centered on a vortex. Foster [26] using constant temperature anemometry in the same tunnel obtained core radii between 0.76 and 1.27 cm (0.3 and 0.5 in.) for comparable vortex strengths. Therefore, there is good reason to believe that there was little interaction between the viscous cores in these cases. Interestingly, the inclination angles obtained from this expression are not very sensitive to the magnitude of the core radius, the axial wavelength, or the order of the ellipse defined by n.

The maximum moment of inertia was used as a representative of the amplitude of motion. In fact, it could be shown that this quantity is related directly to the root-mean squared of the amplitude of motion along the plane containing the predominant motion. The variations of this parameter with downstream position are shown in Fig. 7. In the interest of clarity, not all of the wave numbers are shown in this figure. It is quite evident from the data that in both cases, the amplitude of motion grew with downstream distance, indicating instability. Furthermore, the amplitude appeared to grow with increasing excitation frequency. It is noteworthy that in case 2 where the tunnel speed was slightly higher and the vortices were somewhat weaker, the amplitude appeared to be larger for the same downstream distance and wave number. The growth in the amplitude with downstream distance and with wave number is consistent with the predictions of Miller et al. [20]. Their model also indicated that at lower wave numbers, the symmetric mode would dominate the motion, while at wave numbers above unity, the antisymmetric mode would drive the amplitude. However, attempts at estimating the exponential growth rate a from this data were unsuccessful owing to the scatter in the experimental data.

The spread in the data shown in Fig. 6 prevented any meaningful quantitative comparison of the data with analytical predictions. However, qualitatively, it could be concluded that in the second case, where the vortices were slightly weaker and more unequal in strength, the inclination angles were somewhat smaller. In both cases, averaging the angles over the entire range of wave numbers resulted in values that were very similar to those predicted by Miller et al. However, the scatter in the data, as seen in Fig. 6, rendered the validity of an average value questionable. In each case, out of 24 total points, 8 to 10 points deviated from the mean by more than 1 standard deviation.

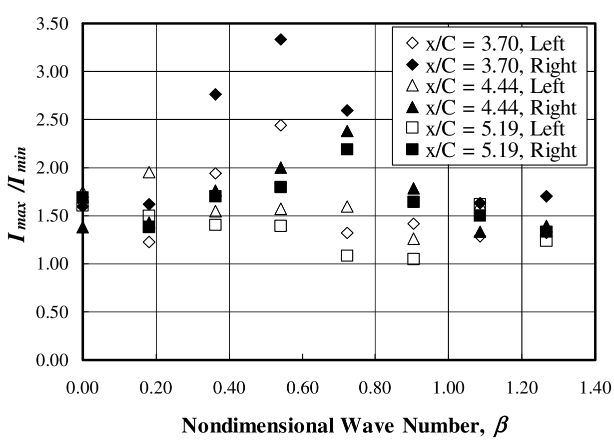

a) Case 1

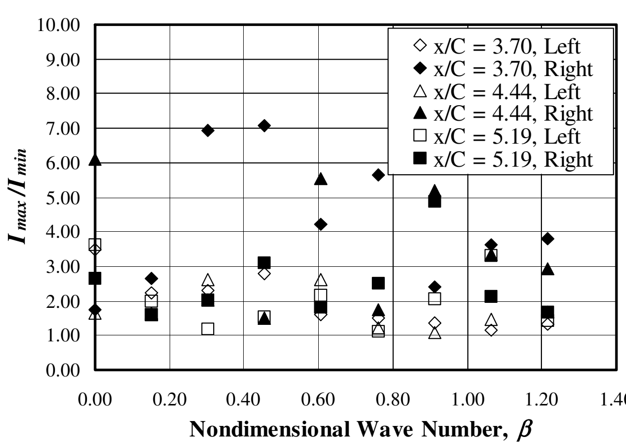

b) Case 2

Fig. 5 Ratio of the second moments of the instantaneous position.

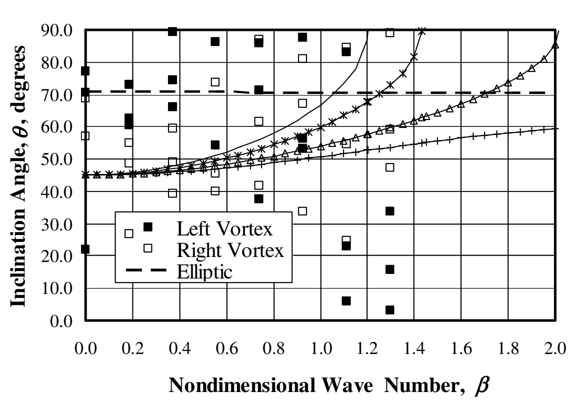

a) Case 1

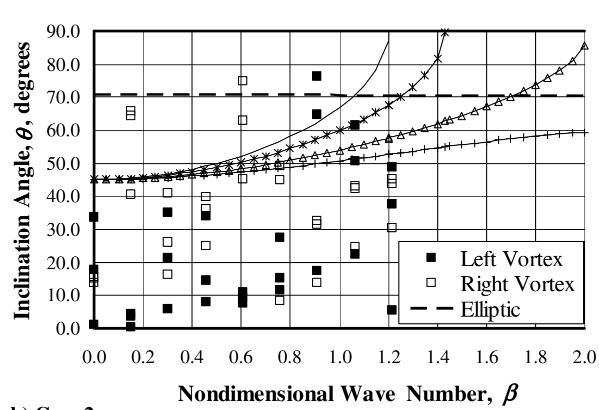

b) Case 2

Fig. 6 Preferred direction of motion. The solid lines are from Fig. 1.

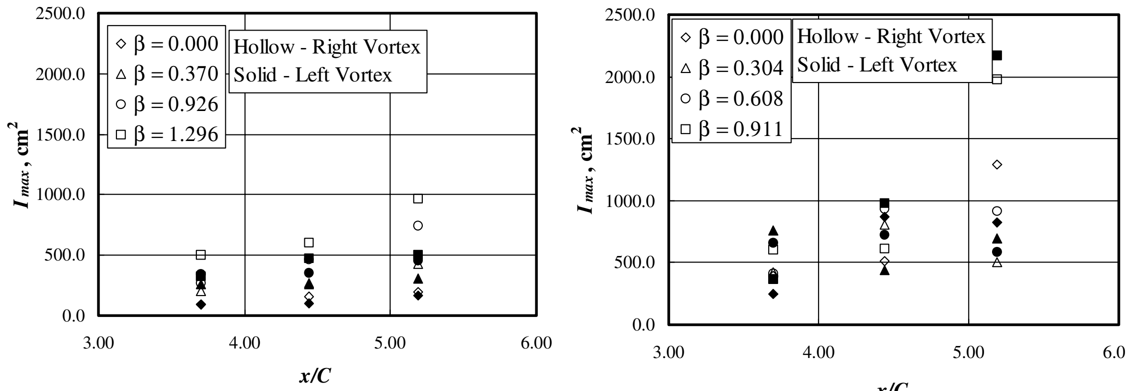

a) Case 1 **b) Case 2**

Fig. 7 Growth of the amplitude of motion with downstream distance.

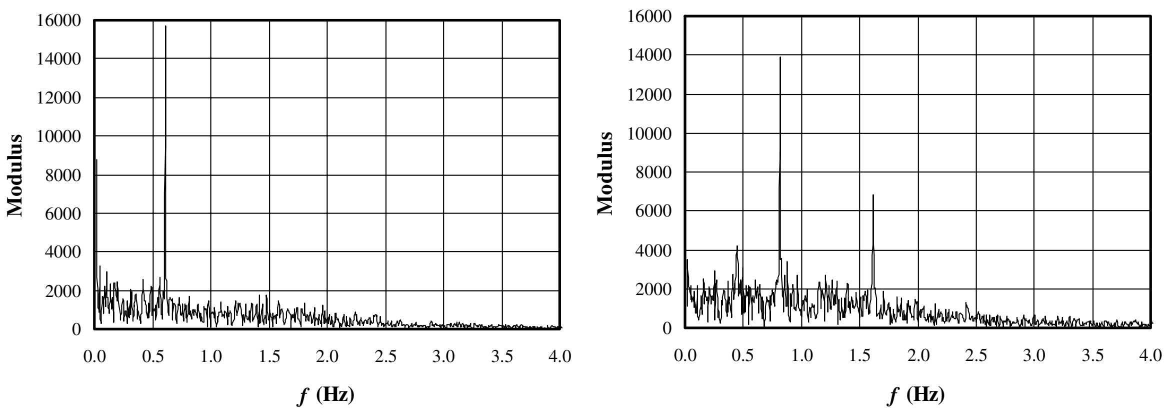

a) Case 1, $f = 0.60$ Hz, $x/C = 4.44$, Right Vortex **b) Case 1, $f = 0.80$ Hz, $x/C = 4.44$, Left Vortex**

Fig. 8 Fourier transform of vertical vortex position time history in units of pixels.

The scatter in the experimental data could be attributed to five sources. The first possibility pertained to the motion of the left vortex. When viewed from a downstream position, the filaments spiraled in the clockwise direction. This caused the left vortex to rise and enter the wake of the left blade, while the right vortex sank and moved away from the right blade. Consequently, the motion of the left vortex was affected by the wake of its blade, resulting in more scatter in its preferred direction of motion.

The second anomaly detected experimentally was the presence of multiple frequencies in the wake. In every case, the excitation frequency could be identified very clearly from the FFT of the vortex position well downstream of the shaker. An example is given in Fig. 8a where the frequency content of the vertical vortex position in pixels clearly shows the excitation frequency. However, because the induced velocity is proportional to the inverse of the radius, when one vortex moves harmonically, its induced velocity contains multiples of its frequency of motion. This can be seen in Fig. 8b where the presence of multiple frequencies is clearly visible. Therefore, even though the excitation was harmonic, the motion of the filaments downstream was not purely harmonic. In fact, this issue calls for a closer examination of the validity of stability analysis in such flow fields via harmonic excitation.

The third source of scatter in the data could be the inequality of the vortices. As explained earlier, the blades' angles of attack had to be adjusted until the center of spiraling appeared visually to be halfway between the filaments. This was a very tedious and inaccurate procedure that sometimes resulted in vortices of unequal strength. Indeed in case 2, the right vortex was approximately 30% weaker than the left vortex (Table 1). However, in the absence of a method that would allow real-time data reduction, the vortex strengths had to be set by trial and error.

The fourth source of error could be the inherent noise in the data acquisition technique and the background noise in the tunnel, both of which could result in the presence of spurious frequencies at the downstream locations. The method, by its design, allowed observation of the dye and not the vortex location. If the dye drifted from the exact core position, its circular frequency would appear as the frequency of motion after the data reduction. However, this behavior was not observed in the case of a single vortex.

Finally, in both of the analytical methods the motion is assumed to be harmonic with small amplitudes for stability analysis. Despite the fact that the excitation frequency could be identified clearly at every downstream location, in reality, the motion was far from harmonic and the amplitude was not necessarily small. Clearly sinusoidal waves were never observed in the water tunnel and the amplitude of motion was large compared with the core radius. Both of these suggest stronger nonlinear effects than could be modeled by an exponential stability analysis technique.

Even though the spread in the experimental data prevented quantitative comparison of the data with analytical predictions, these results demonstrated all of the essential features of such flowfields. The information presented here was not filtered and contained *all* of that obtained experimentally. These data clearly showed that the dynamic interactions between corotating vortex filaments lead to an unstable oscillatory motion with a distinct preferred direction.

Conclusions

The dynamic interactions of pairs of corotating vortex filaments were explored experimentally. The investigations were performed in a water tunnel and the time history of the motion of the filaments was recorded. Two sets of data were presented in which the filaments were excited over a wide range of frequencies using a shaker. The time-dependent motion was shown to be unstable, resulting in growing amplitude, consistent with analytical predictions. Also, the motion exhibited a preferred direction implying the tendency of the filaments to form planar waves, inclined relative to the surface connecting them. The angles of the planes containing these waves were measured and were compared to the values predicted analytically. Although the scatter in the experimental data prevented quantitative comparison with the analytical results, all of the essential features predicted by the analytical models were shown to be present in the flow.

In light of the lack of conclusive agreement between the analytical models and the experimental data, there seems to be a need for further investigation of this type flow. Three possibilities come to mind at this point. The first is to gather further experimental data. The present paper contains the results of only two sets of data. Indeed, more data are needed for a comprehensive statistical analysis of the results. The second option would be to repeat the same experiments with a different setup, such as a wing and a flap or two opposing wings. This approach would allow identification of the contribution of the present setup to the dynamics of the flow. Finally, efforts are underway in the area of computational modeling. The authors hope that CFD models can shed more light on the nature of this type of flowfield.

References

[1] Laporte, F., and Corjon, A., "Direct Numerical Simulations of the Elliptic Instability of a Vortex Pair," *Physics of Fluids*, Vol. 12, No. 5, May 2000, pp. 1016–1031.

[2] Haverkamp, S., Neuwerth, G., and Jacob, D., "Studies on the Influence of Outboard Flaps on the Vortex Wake of a Rectangular Wing," *Aerospace Science and Technology*, Vol. 7, No. 5, 2003, pp. 331–339.

[3] Crouch, J. D., "Instability and Transient Growth for Two Trailing-Vortex Pairs," *Journal of Fluid Mechanics*, Vol. 350, No. 1, 1997, pp. 311–330.

[4] Fabre, D., Jacquin, L., and Loof, A., "Optimal Perturbations in a Four-Vortex Aircraft Wake in Counter-Rotating Configuration," *Journal of Fluid Mechanics*, Vol. 451, Jan. 2002, pp. 319–328.

[5] Dritschel, D. G., and Legras, B., "The Elliptical Model of Two-Dimensional Vortex Dynamics, II: Disturbance Equations," *Physics of Fluids*, Vol. 3, No. 5, May 1991, pp. 855–869.

[6] Meunier, P., Ehrenstein, U., Leweke, T., and Rossi, M., "A Merging Criterion for Two-Dimensional Co-Rotating Vortices," *Physics of Fluids*, Vol. 14, No. 8, Aug. 2002, pp. 2757–2766.

[7] Le Dizès, S., and Verga, A., "Viscous Interactions of Two Co-Rotating Vortices Before Merging," *Journal of Fluid Mechanics*, Vol. 467, Sept. 2002, pp. 389–410.

[8] Meunier, P., and Villermaux, E., "How Vortices Mix," *Journal of Fluid Mechanics*, Vol. 476, Feb. 2003, pp. 213–222.

[9] Bertenyi, T., and Graham, W., "An Experimental Study of the Merging of Aircraft Wake Vortices," AIAA Paper AIAA-2000-4129, 2000.

[10] Meunier, P., and Leweke, T., "Three-Dimensional Instability During Vortex Merging," *Physics of Fluids*, Vol. 13, No. 10, Oct. 2001, pp. 2747–2750.

[11] Le Dizès, S., and Laporte, F., "Theoretical Predictions for the Elliptical Instability in a Two-Vortex Flow," *Journal of Fluid Mechanics*, Vol. 471, Nov. 2002, pp. 169–201.

[12] Laporte, F., and Leweke, T., "Elliptic Instability of Counter-Rotating Vortices: Experiment and Direct Numerical Simulation," *AIAA Journal*, Vol. 40, No. 12, Dec. 2002, pp. 2483–2494.

[13] Cerretelli, C., and Williamson, C. H. K., "The Physical Mechanism For Merging of Trailing Vortices," AIAA Paper 2003-1287, 2003.

[14] Haverkamp, S., Neuwerth, G., and Jacob, D., "Active Control of Aircraft Vortex Wakes by Means of Preset Ailerons," AIAA Paper 2003-6823, 2003.

[15] Hassan, A., "Motion of Three Vortices," *Physics of Fluids*, Vol. 22, No. 3, March 1979, pp. 393–400.

[16] Eckhardt, B., "Integrable Four Vortex Motion," *Physics of Fluids*, Vol. 31, No. 10, Oct. 1988, pp. 2796–2801.

[17] Saffman, P. G., *Vortex Dynamics*, Cambridge Univ. Press, New York, 1997.

[18] Jimenez, J., "Stability of a Pair of Co-Rotating Vortices," *Physics of Fluids*, Vol. 18, No. 11, Nov. 1975, pp. 1580–1581.

[19] Crow, S. C., "Stability Theory for a Pair of Trailing Vortices," *AIAA Journal*, Vol. 8, No. 12, Dec. 1970, pp. 2172–2179.

[20] Miller, T. S., Kliment, L. K., and Rokhsaz, K., "Dynamics of Co-Rotating Vortex Filaments—Part 1: Analytical Mode," *Journal of Aircraft*, Vol. 43, No. 5, 2006, pp. 1434–1439.

[21] Jacob, J. D., "Experimental Investigation of Co-Rotating Trailing Vortices," AIAA Paper 98-0590, 1998.

[22] Jacob, J. D., "Experiments on Trailing Vortex Merger," AIAA Paper 99-0547, 1999.

[23] Jacob, J. D., and Savas, O., "Vortex Dynamics in Trailing Wakes of Flapped Rectangular Wings," AIAA Paper 97-0048, 1997.

[24] Kliment, L. K., "Experimental Investigation of Flap Tip and Wing Tip Vortex Interactions," M.S. Thesis, Wichita State University, Wichita, KS, Dec. 2002.

[25] Rokhsaz, K., and Kliment, L. K., "Experimental Investigation of Co-Rotating Vortex Filaments in a Water Tunnel," *Journal of Aircraft*, Vol. 40, No. 6, Nov.–Dec. 2003, pp. 1115–1122.

[26] Foster, S. R., "Exploratory Study of an Aircraft Wake Vortex Filament in a Water Tunnel," M.S. Thesis, Aerospace Engineering, Wichita State University, Wichita, KS, Dec. 1999.

[27] Rokhsaz, K., Rebours, R., and Foster, S. R., "Quantitative Measurements of Wake Vortex Motion in a Water Tunnel," *Journal of Aircraft*, Vol. 39, No. 5, Sept.–Oct. 2002, pp. 862–867.